Arthritis Research & Therapy

RESEARCH

Open Access

Integrative metabolomic-proteomic analysis uncovers a new therapeutic approach in targeting rheumatoid arthritis

Prachi Agnihotri[1,2], Mohd Saquib[1,2], Lovely Joshi[1,2], Swati Malik[1,2], Debolina Chakraborty[1,2], Ashish Sarkar[1,2], Uma Kumar[3] and Sagarika Biswas[1,2*]

Abstract

Objective Rheumatoid arthritis (RA) is a chronic inflammatory condition that, despite available approaches to manage the disease, lacks an efficient treatment and timely diagnosis. Using the most advanced omics technique, metabolomics and proteomics approach, we explored varied metabolites and proteins to identify unique metabolite-protein signatures involved in the disease pathogenesis of RA.

Methods Untargeted metabolomics ($n=20$) and proteomics ($n=60$) of RA patients' plasma were carried out by HPLC/LC-MS/MS and SWATH, respectively and analyzed by Metaboanalyst. The targets of metabolite retrieved by PharmMapper were matched with SWATH data, and joint pathway analysis was carried out. An in-vitro study of metabolites in TNF-α induced SW982 cells was conducted by Western, RT-PCR, scratch, and ROS scavenging assay. The effect of GUDCA was also evaluated in the CIA rat model.

Results A Total of 82 metabolites and 231 differential proteins were revealed. Porphyrin and chlorophyll pathway and its metabolite Glycoursodeoxycholic acid (GUDCA) was found to be significantly altered. In vitro analysis has shown that GUDCA reduces inflammation thus offering protection against ROS production and cell proliferation. PharmMapper analysis revealed that GUDCA was significantly linked with identified SWATH proteins insulin like growth factor-1(IGF1), and Transthyretin (TTR) and it upregulates the expression of IGF1 and downregulates the expression of TTR in both in vitro and in vivo models.

Conclusion GUDCA was found to possess antioxidative, antiproliferative properties and an effective anti-inflammatory property at a low dosage. It may be considered as a potential therapeutic option for reducing the inflammatory parameters associated with RA.

Keywords Rheumatoid arthritis (RA), Metabolomics, Metabolites, Proteomics, SWATH, Inflammatory pathways, CIA-Rat model

*Correspondence:
Sagarika Biswas
sagarika.biswas@igib.res.in

Full list of author information is available at the end of the article

Graphical Abstract

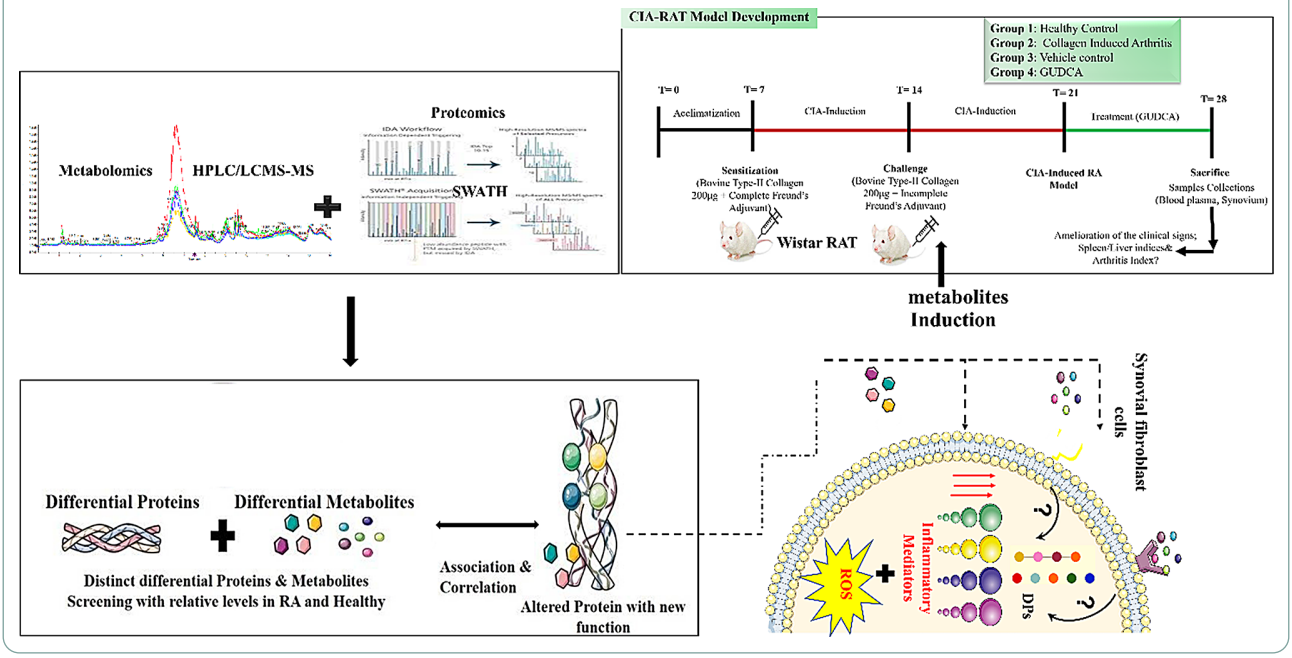

Introduction

Rheumatoid arthritis (RA) is an autoimmune systemic disorder characterized by persistent inflammation resulting in the destruction of synovium, bone, and cartilage [1]. Multiple external/internal factors, including epigenetic, genetic, and environmental factors, trigger heterogeneous pathogenicity during disease progression [2]. The epidemiology of RA suggests its occurrence in nearly 5 per 1000 adults worldwide, and women are 2 to 3 times more prone to its development than men. Despite the availability of drugs and treatments, the insufficient diagnosis/prognosis led to improper treatment, resulting in the threatening aspects of the disease [1]. Various markers are used to diagnose this disease, often lacking sensitivity and specificity [3], and overlap with other similar diseases. Therefore, a definitive study of the prognosis and detection of the disease is required.

Currently, the omics approach, expanding its roots to metabolomic tools is in demand to determine the directional changes of altered metabolism in disease to understand the molecular pathophysiology of the disease [4, 5]. The range of these metabolic alterations and various altered molecules, such as metabolites and proteins, could be prominent markers of cytokine-mediated inflammatory processes in RA. Metabolomics, an emerging tool, has been recently employed to identify potential markers in multiple diseases, such as infectious diseases, cancer, inflammatory diseases, and coronary artery disease (CAD) [6].

Metabolites are small molecules formed as by-products from multiple metabolic pathways. Generally, these metabolites get al.tered much earlier than the onset of diseases; hence, identification of altered metabolites holds significant potential in associating genes and proteins in a disease state [6]. In contrast to genomics and proteomics, the focus of metabolomics is on connecting small molecules of biological pathways that are modulators of genes and proteins' activity, allowing more precise identification of disease-associated phenotypes occurring within the biological system [7].

It is reported that metabolites are the responses of rapid physiological actions according to the disease activity. To manage numerous cellular processes and to regulate protein activities, interactions between proteins and metabolites are essential [8]. Reports have indicated that metabolic enzymes, transcription factors, transporters, and membrane receptors can be controlled by interactions with proteins and metabolites (PMIs) [9].

Therefore, we used a proteomic approach apart from metabolomics to identify the significantly differential proteins in RA plasma samples. Differential proteome profiling is a powerful tool for studying proteins and their alterations in specific disease conditions, providing various differentially expressed proteins (DEPs) associated with disease development [10]. Further, the integrated analysis of metabolite-protein interactome has been reported to characterize any biological process efficiently [4].

Therefore, we focused our attention on identifying novel differential metabolites linked to differential proteome profile of RA and explored their relationship and relative importance in determining disease severity.

Plasma samples of RA patients and healthy control (HC) were used in our study to identify differential metabolites and proteins via HPLC-MS/MS and SWATH-MS analysis, respectively, followed by in-silico analysis to identify altered pathways. Relative expression of the metabolite-induced protein was validated in RA synovial fibroblast cells (SW982) through in vitro studies. This was followed by in vivo validation using a Collagen Induced Arthritis (CIA) rat model. In this study, Glycoursodeoxycholic acid (GUDCA) metabolite was identified as a prominent regulatory metabolite in RA. Upon treatment with GUDCA, it was found that there was an increased expression of IGF1, and a decreased expression of TTR, and the treatment had anti-inflammatory, antioxidative, and antiproliferative properties. GUDCA may, therefore, be considered a therapeutic potential molecule for RA.

Materials and methods

Clinical samples

Blood samples ($n=60$) were collected from RA patients from the Department of Rheumatology, All India Institute of Medical Sciences (AIIMS), New Delhi, India [11]. Similarly, blood samples ($n=40$) were collected from HC with no prior ailment and joint inflammation. The medical history of each patient was collected (Supplementary Table 1) [12]. See details in supplementary file).

Metabolomics analysis

To analyze the differential metabolites, HPLC-MS/MS was carried out using RA ($n=20$) and HC ($n=20$) plasma samples. Two complimentary LC-MS/MS metabolomics methods were applied: HILIC and C18 chromatography. The raw LC-MS (.wiff files) data file was analysed by Peak View (ABSciex). Fold change criteria was considered to categorize upregulated (fold change ≥ 1.5) and downregulated (fold change ≤ 0.5) metabolites, respectively, and p-value < 0.05 was considered [13, 14]. (See details in supplementary file).

Proteomics of plasma samples: SWATH-MS acquisition

Plasma samples of RA ($n=60$) and HC ($n=40$) were taken, and a total of 70 µg protein was estimated by BCA and digested overnight at 37 °C with 0.1 µg/µl trypsin (Promega, USA) [12, 15]. (See details in supplementary file).

Integration of metabolomics and proteomics

Association analysis between metabolomics and proteomics data was performed using significant differential metabolites and protein profiles between RA and HC groups. Joint Pathway Analysis was carried out using MetaboAnalyst 5.0 (https://www.metaboanalyst.ca/). It enabled us to visualize significant genes and metabolites that were enriched in a particular pathway and integrated the underlying relationships among differentially expressed metabolites and proteins [16].

Target Prediction of metabolites

The major concern in drug discovery is to validate the best-screened active compounds' interaction with appropriate targets [17]. To identify the potential molecular targets of the screened metabolites, PharmMapper server database (http://lilab.ecust.edu.cn/PharmMapper) was used [18, 19]. The gene targets were matched with protein profile identified by SWATH analysis. (See details in supplementary file)

Western blot (WB) and enzyme-linked immunosorbent assay (ELISA)

For WB analysis, 4 pooled plasma proteins of RA and HC were used. Each pooled sample consists of RA ($n=10$) and HC ($n=10$); thus, 40 RA and 40 HC samples were used, and 20 µg of pooled plasma proteins were run on SDS-PAGE and anti-IGF1 (Santa Cruz, USA) (1:2000) as the primary antibody and anti-mouse (1:5000) as a secondary antibody were used. The indirect ELISA was performed using diluted (1 µl/200µl) RA plasma ($n=60$) and HC ($n=40$), coated into 96-well micro-titer plates (Thermo Scientific, Nunc, USA), followed by incubation with primary antibody (Anti-IGF1) and secondary antibody (anti-mouse). The absorbance was observed at 495 nm [12, 20]. (See details in supplementary file).

Peripheral blood mononuclear cell (PBMC) isolation, RNA isolation, WB, and qRT-PCR

PBMCs are the primary immune cells in the human body and offer discriminatory immune responses toward inflammation [5]. PBMCs were isolated by centrifuging RA blood ($n=6$) and HC ($n=6$) using histopaque reagent [20] and then used to perform WB with 3 pooled RA and HC samples, respectively ($n=2$ in each pooled sample) [15]. Total RNA was extracted from PBMCs of HC ($n=6$) and RA ($n=6$) using Tri-Xtract Reagent (G-biosciences). GAPDH as an internal reference. Primers are shown in Supplementary Table 2 (See details in the supplementary file). Similarly, in our earlier study, protein and mRNA levels of TTR were checked in PBMCs of RA blood [20].

Correlation analysis

The association of GUDCA levels with RA disease activity, specifically with ACCPA and DAS28-ESR scores was investigated [20, 21]. Additionally, the relationship between IGF1 levels, (measured by ELISA), and RA

disease activity (assessed by the DAS28-ESR score) was examined. (See details in the supplementary file)

In-Vitro analysis

Human synovial fibroblast SW982 cell culture and MTT test

SW982 cells were cultured in DMEM media and treated with GUDCA metabolite (1–70μM range) for 24 h in serum-free media [22]. Absorbance was measured at 540 nm. See details in the supplementary file)

Total protein extraction and western blotting

SW982 cells were cultured and pre-treated with GUDCA (50μM- 6.25 μM) for 24 h. Protein was extracted in RIPA buffer after 10 min induction with TNF-α (10ng/ml) [23]. The blot was incubated with anti-p65, anti-IGF1, and anti-TTR separately as primary antibodies [22]. (See details in supplementary file)

Real-time quantitative reverse transcription PCR (qRT-PCR)

SW982 cells were cultured and incubated with GUDCA (50μM) for 24 h. The effect was investigated by TNF-α treatment (10 ng/ml) on GUDCA pretreated cells for 1 h. Total RNA was isolated and subjected to cDNA preparation, and mRNA expression was evaluated and quantitated using $2^{-\Delta\Delta CT}$ formula [22]. Human-specific primer sequences are shown in Supplementary Table 2. (See details in supplementary file)

Scratch assay analysis

SW982 cells were grown in a culture plate, the vertical scratch was drawn, and each scratch area was measured before and after the treatment with GUDCA (50μM). Bright-field images were taken at 0 h and 48 h and analyzed using a Nikon Eclipse 650 (NIKON, Tokyo, Japan) at ×10 magnification. The images were analyzed using ImageJ software [24]. (See details in supplementary file)

Total reactive oxygen species (ROS) estimation

SW982 cells were pretreated with GUDCA (50μM) with and without TNF-α (24 h), followed by adding 10μM working solution of DCFH-DA into each well for 30 min. Fluorescence images were taken by ZOE Fluorescent Cell Imager and analyzed by ImageJ software [22]. (See details in supplementary file)

In vivo studies

Development of collagen-induced arthritis (CIA) rat model

Female Wistar rats (60–80 g) were procured from the ICMR -National Institute of Nutrition in Hyderabad, India. The work design was approved by the Institute's Animal Ethical Committee (IGIB/IAEC/3/3/Mar 2023). The animals were randomly divided into four groups (n=4). The untreated group/ healthy control (HC) (Group 1), Collagen-Induced Arthritis (CIA) (Group 2), vehicle control (VC+CIA) (Group 3), and GUDCA treated (CIA+GUDCA) (Group 4). CIA rats (Except the HC group) were then induced with 2 mg/ml collagen (Type II) from chicken (Sigma, USA). GUDCA was administered at 800 μg/Kg of rat body weight mixed with corn oil/ benzyl alcohol (95:5 v/v) and was injected subcutaneously [25, 26]. (See details in supplementary file)

Measurement of CIA induction in experimental groups and detection of RA

Throughout the study, paw volume and arthritis index (AI) were assessed in individual animals to monitor disease progression from day 0th to day 28th [27]. Splenic index and liver index were calculated for each rat as the ratio of the spleen/liver: body weight [28]. (See details in supplementary file)

Enzyme-linked immunosorbent assay (ELISA) of cytokines in plasma

Rat plasma was separated and added (100 μl) to the pre-coated ELISA plate, followed by the manufacturer's guidelines. TNFα, IL(Interleukin)1β, and IL-6 cytokines were quantified using ELISA kits (ELK Biotechnology, China) [12].

Hematoxylin and eosin staining (H & E)

Rat synovium was sliced and fixed in 10% formalin, fixed in the paraffin block, sliced (5 μm thick) using a microtome, and slides were prepared. Slides were viewed under a Nikon microscope. Images of the slides at 10X magnification were taken, and Image-J software was used to analyze the images [25] (See details in supplementary file).

Western blot analysis of the CIA model rat plasma

The blood samples were drawn through direct heart puncture and collected in EDTA coated vacutainer tubes (BD, Franklin Lakes, NJ, USA), and plasma was separated. Similarly, synovial tissue was collected and crushed in liquid nitrogen from each rat, and the lysate was prepared in RIPA buffer and centrifuge; further supernatant was stored at -80 °C for further analysis. For WB analysis, the total protein (10 μg) concentration was run on the gel as mentioned above [29] (See details in supplementary file).

Enzyme-linked immunosorbent assay (ELISA) of synovium

The indirect ELISA was performed using synovium lysate of all groups diluted (10 μl/90μl) with coating buffer into 96-well micro-titer plates (Thermo Scientific, Nunc, USA) and incubated overnight at 4°C and proceeded as mentioned above [29] (See details in supplementary file).

Statistical analysis

All non-parametric Mann–Whitney tests were performed using Graph pad Prism 9.0. The complete data set was analyzed using MetaboAnalyst 3.0. Pathway enrichment analysis was performed to find the related pathway with the altered metabolites. Statistical analysis was performed with the paired student's t-test to compare the data between two groups, and ANOVA was used to compare data among multiple groups. The obtained p-values were represented by asterisks on the graph (*$p \leq 0.05$, **$p \leq 0.01$, ***$p \leq 0.001$, ****$p \leq 0.0001$). Each experiment was repeated at least three times.

Results

Identification of differentially expressed metabolites in RA plasma

Using HPLC-MS/MS, a total of 2519 m/z (mass/charge ratio) were identified in RA plasma and represented by volcano plots. (Fig. 1A) Among them, 685 m/z were found to be differentially regulated, 70 m/z were upregulated (Blue dots) and 47 m/z (green dots) were downregulated. (Fig. 1B). The differentially regulated metabolites were further processed with the metabolomics library, from which 82 were annotated (Supplementary Table 3) with high confidence. Amongst these, 23 metabolites were found to be significantly regulated (7 downregulated and 2 upregulated), as depicted in the pictorial representation (Fig. 1C) (Table 1). A threshold of fold change criteria for upregulated (fold change ≥ 1.5) and downregulated (fold change ≤ 0.5) was considered for the identification of differential metabolites.

Analysis of differential metabolites

For the discriminant analysis of RA and HC, 82 annotated metabolites were opted for the OPLS-DA and PCA, used to recognize group differences. The analysis was normalized using Pareto scaling. 2D score plot of OPLS-DA analysis (Fig. 1D) shows a T score of 8% (variation between the groups) and an orthogonal T score of 12.4% (variation within the groups). The 3D score plot of PCA was generated, which showed the differential pattern of metabolites (Fig. 1E). Principal components (PC) PC1, PC2, and PC3 accounted for 22.6%, 13.2%, and 11.2% of the total variance, respectively, indicating that the metabolites of RA samples were distinctly discriminated from the healthy samples. A variable importance projection (VIP) score plot was created to recognize the top discriminators, and 15 top metabolites of RA were revealed (Fig. 1F). To figure out the most classified significant metabolites, the criteria of VIP values were set to 2 to obtain pre-selected metabolites. This clarifies the variance described by the top-tiered metabolites among RA and healthy groups.

Pathway enrichment analysis of metabolites

Pathway enrichment analysis depicts the changes in the patterns of metabolite concentration biologically and identifies the pathways that impact the metabolite pattern. We used Metaboanalyst 3.0 and revealed that altered metabolites were associated with Starch and sucrose, galactose, Porphyrin, and Phenylacetate metabolism. (Fig. 1G) Pathway enrichment ratios were also calculated by Metaboanalyst and visualized by bar graph. (Fig. 1H)

Identification of differentially expressed proteins (DEPs) in RA plasma

A total of 231 proteins were identified by SWATH-MS analysis (Supplementary Table 4), depicted by the volcano plot. Amongst, 62 proteins (violet spots) were identified as significant DEPs in RA compared to control samples (Fig. 2A), 29 out of 62 DEPs were upregulated (red spots), and 23 were downregulated (green spots) (Fig. 2B and C) (Table 2). A threshold of fold change criteria for upregulated (fold change ≥ 1.5) and downregulated (fold change ≤ 0.5) was considered significant for identified DEPs between the groups.

Joint pathway analysis of differential protein and metabolite profile

Joint pathway analysis is an integrative analysis to assess the commonly associated pathways between the differential profile of metabolites and proteins of RA patients. Differentially expressed proteins and metabolites significantly enriched in Arachidonic acid metabolism, porphyrin and chlorophyll metabolism, Aminoacyl-tRNA biosynthesis, glyoxylate and dicarboxylate metabolism, and phenylalanine pathways and were found to be interrelated with identified differential proteins and metabolites (Fig. 2D).

ACCPA analysis

ACCPA levels are directly proportional to disease severity [30]. In this study, ACCPA levels analyzed in plasma from individuals with RA to establish the relationship between ACCPA and GUDCA levels. Results suggested significantly higher levels of ACCPA in RA patients compared to the HC (Fig. 2E).

Comparative analysis of DEPs with differential metabolites and their relation with RA

In the analysis, "Porphyrin metabolism" was found to be a significant pathway associated with RA. This pathway involved three identified metabolites (Glycocholic acid, Glycodeoxycholic acid, and Glycoursodeoxycholic acid), with Glycoursodeoxycholic acid (GUDCA) being a significantly downregulated metabolite (0.44-fold change). GUDCA was found to have a significant moderate

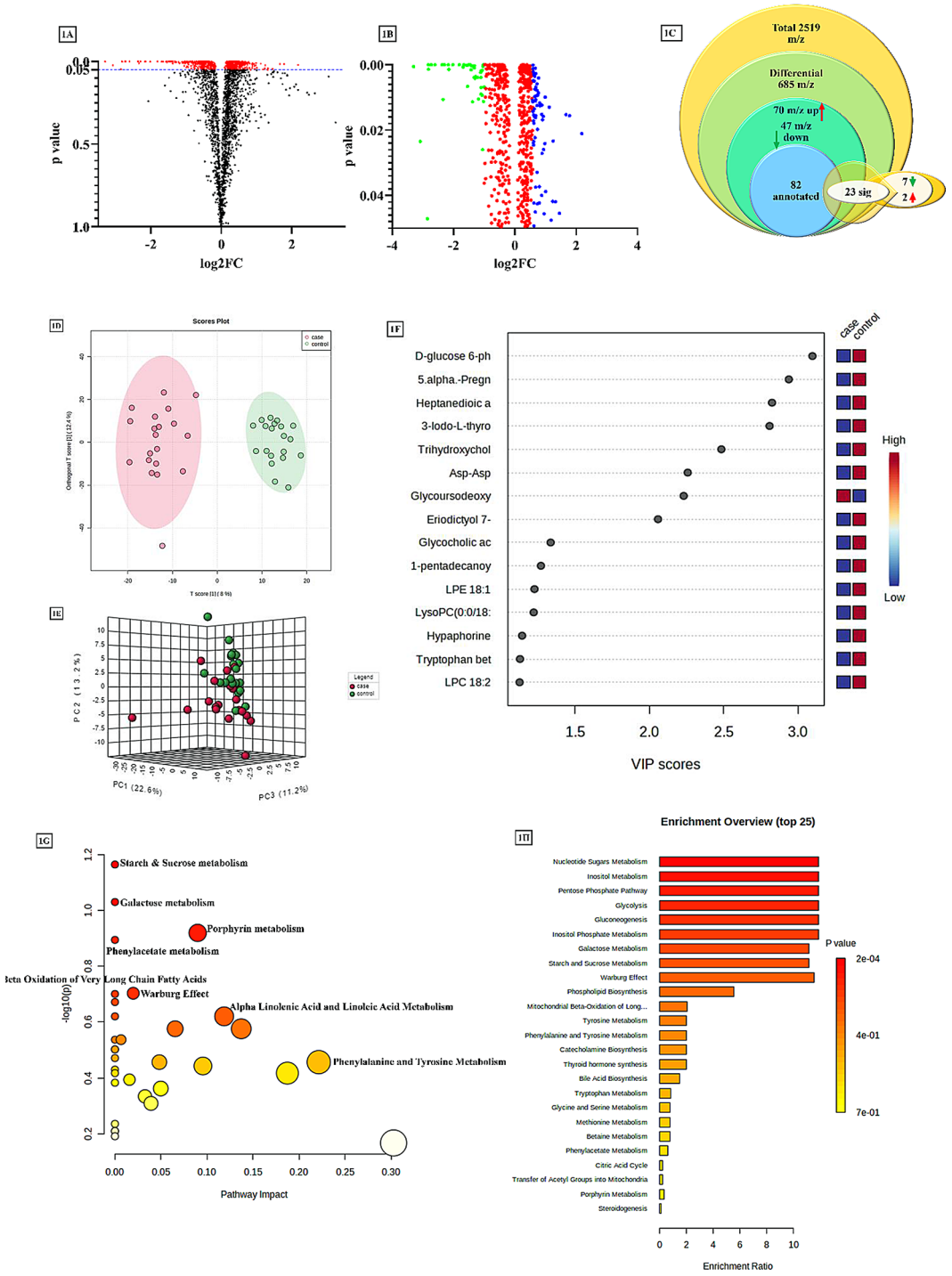

Fig. 1 (**A**) Volcano plot showing altered metabolite features in the test set of RA and controls (fold change ≥ 1.5, fold change ≤ 0.5, $p < 0.05$). A total of 2519 m/z was plotted with 685 m/z significantly regulated metabolites (red dots). (**B**) Graph depicting 70 significantly upregulated m/z (Blue dots) and 47 significantly downregulated (Green dots) m/z. (**C**) Pictorial representation of identified m/z downstream analysis with their significance level. Log2FC; log2 fold change, m/z; mass to charge ratio. Multivariate analysis (**D**) 2D score plot showing the distinct distribution of RA cases and controls in the validation set as discriminated by the identified altered metabolites using OPLS-DA analysis. (**E**) 3D plot showing the distinct distribution of RA cases and controls using PCA analysis. (**F**) Variable importance in projection (VIP) plot depicting the top 15 discriminators for RA cases in the validation set. (**G**) Pathway analysis of identified metabolite set by metaboanalyst 5.0 H) Pathway enrichment analysis represented by Bar graph computing a single P value for each metabolic pathway. PC; principal component, VIP; variable importance in projection, OPLS-DA; Orthogonal partial least squares-discriminant analysis, RA; rheumatoid arthritis, HC; healthy control

Table 1 List of metabolites annotated with high confidence in which 23 metabolites were differentially regulated by NIST library and MS-Dial 5.0

S.No.	m/z	Metabolite	Fold change	*p* value
1	538.3154	Cholylmethionine	3.177627	0.015285
2	566.3472	LPC 18:1	1.51379	0.051561
3	165.0999	6-Pentyl-2 H-pyran-2-one	1.326574	0.034463
4	496.331	LPC 16:0	0.829247	0.035057
5	454.2848	1-palmitoyl-2-hydroxy-sn-glycero-3-phosphoethanolamine	0.780522	0.036636
6	790.5701	PC O-38:7	0.768475	0.046717
7	544.3292	LPC 20:4/0:0	0.757545	0.002489
8	246.1643	CAR 5:0	0.722267	0.015927
9	520.3286	LPC 18:2	0.707948	5.45E-05
10	524.363	LysoPC(0:0/18:0)	0.704678	0.024745
11	488.2879	GLYCOCHOLATE	0.685498	0.038619
12	786.591	1,2-dioleoyl-sn-glycero-3-phosphatidylcholine	0.670958	0.01464
13	482.3144	1-pentadecanoyl-2-hydroxy-sn-glycero-3-phosphocholine	0.657604	0.013365
14	480.2975	LPE 18:1	0.631667	0.000649
15	449.3838	Trihydroxycholestanoic acid	0.520398	0.007314
16	595.1513	Eriodictyol 7-O-neohesperidoside	0.500863	0.036249
17	258.9185	D-glucose 6-phosphate	0.490946	0.011213
18	246.9637	Asp-Asp	0.485635	0.000563
19	478.2915	1-Oleoyl-sn-glycero-3-phosphoethanolamine/LysoPE(18:1/0:0)	0.481877	0.02599
20	238.9864	Heptanedioic acid, 1-(2-cyclopentylidenehydrazide)	0.466123	0.006953
21	448.3038	Glycoursodeoxycholic acid	0.449878	0.007679
22	413.5848	5.alpha.-Pregnan-3.alpha.,17-diol-20-one 3-sulfate	0.367392	3.79E-06
23	464.2986	Glycocholic acid	0.197437	0.010649

m/z; mass by charge ratio

negative correlation with ACCPA concentration (Fig. 2F) and DAS28-ESR activity score (Fig. 2G). As a result, it was chosen for further analysis (Supplementary Table 3). The PharmMapper database predicted 300 gene targets of GUDCA metabolite (Supplementary Table 5). These target genes were first matched with DisGeNET database genes of RA. Then the common genes were matched with identified proteins in RA plasma by SWATH (Supplementary Table 4) to deduce the potential metabolite-protein pair altered in RA (Supplementary Table 6). This comparative analysis revealed that IGF1, TTR, and SHBG were common target proteins of GUDCA. However, IGF1 and TTR were screened and selected for further study in RA condition based on their GDA score, which was found to be 0.05 and 0.02, respectively, and was also found to be significantly (0.42-fold) downregulated and upregulated (1.89-fold) respectively in SWATH data. (Supplementary Table 4)

Validation of target protein expression

The expression of significantly differential target protein (IGF1) was validated in four pooled samples of RA and HC by WB. The densitometric analysis showed a significant downregulation of IGF1 level ($p<0.0349$) in RA compared to HC (Fig. 3A), with a 1.6-fold change after normalization with total protein. Further, ELISA revealed a 1.2-fold significantly downregulated expression of IGF1 ($p<0.011$) in RA plasma ($n=60$) compared to HC ($n=40$) (Fig. 3B). The levels of IGF1 were found to have a significant negative correlation with DAS28-ESR (Fig. 3C). Similar IGF1 levels were confirmed in PBMCs of RA and found to be 3-fold downregulated ($p<0.0007$) at the protein level by WB and 1.5-fold downregulated ($p<0.0001$) at levels by qRT-PCR, compared to HC after normalization with β-actin used as a loading control. (Figure 3D and E). Similarly, the levels of TTR's protein and mRNA levels were verified in RA plasma and PBMCs, compared to HC, in our previous studies [20].

Human synovial fibroblast (SW982) cytotoxicity analysis of GUDCA

Cell viability of human synovial fibroblast cells (SW982) pre-treated with GUDCA (1–70 μM/ml) was measured by MTT (Fig. 4A). The bar represented the percentage (%) of cell survivability after the induction of cells. The results showed that less than 50μM GUDCA concentration did not affect cell viability.

Effect of GUDCA on inflammatory condition and target proteins

The expression level of NFκB/(p65), a prominent inflammatory mediator, was analyzed and validated in 24 h pre-treated SW982 cells with GUDCA (range of 50μM-6.25μM) followed by TNF-α (10ng/ml) induction for

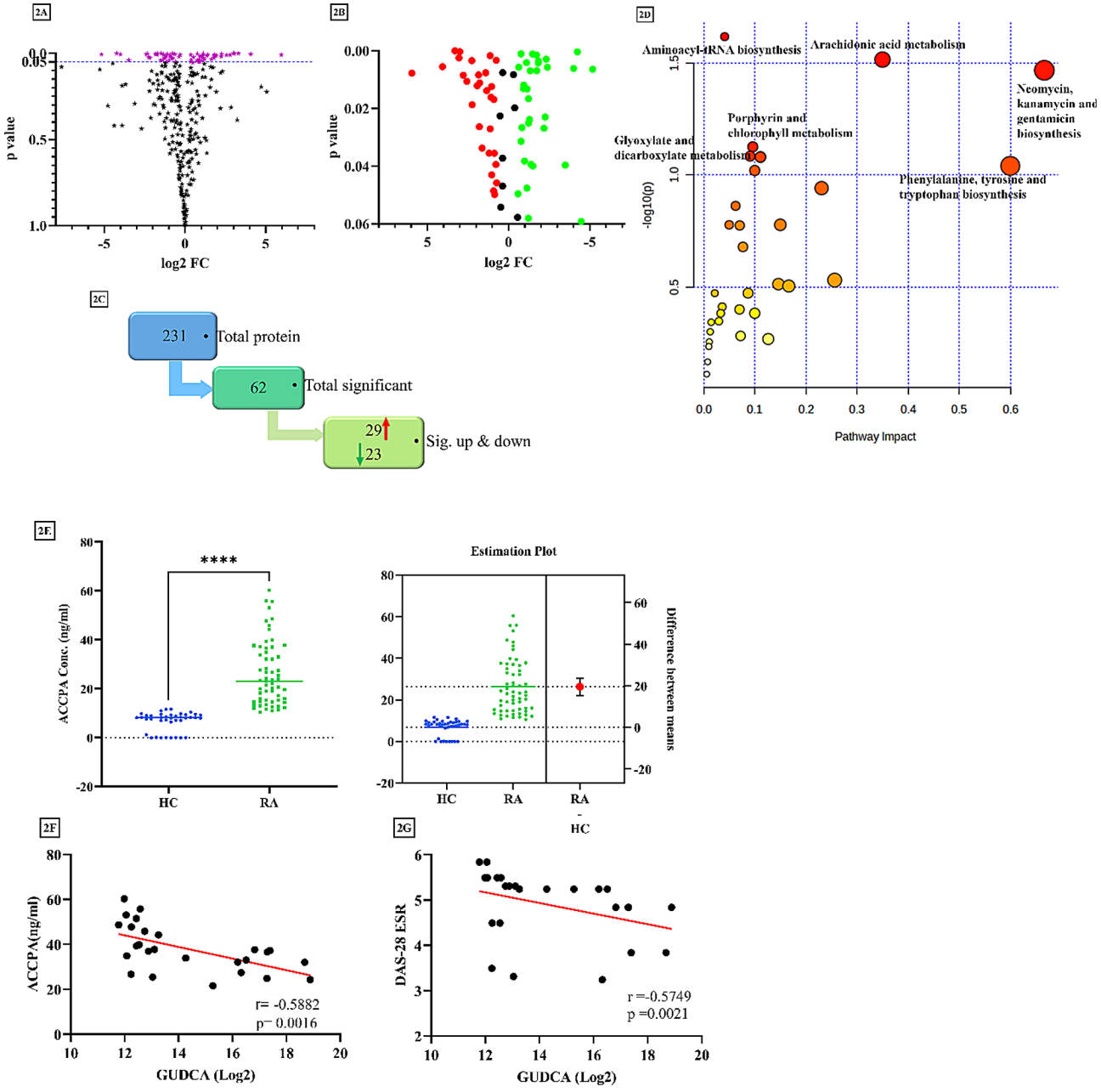

Fig. 2 Proteomic analysis by SWATH (**A**) Volcano plot showing altered proteins in the test set of RA and HC (fold change ≥ 1.5, fold change ≤ 0.5, $p < 0.05$), A total of 62 significant proteins were represented by purple dots (**B**) Graph depicting 29 significantly upregulated (red dots) proteins and 23 significantly downregulated proteins (green dots), rest proteins significant but did not fall under the selection criteria (Black dots) (**C**) Pictorial representation of identified protein shown downstream analysis with their significance level (**D**) Joint pathway analysis of identified metabolites and proteins by metaboanalyst. (**E**) Significant difference in ACCPA levels in RA ($n = 60$) and HC ($n = 40$) samples with estimation plot. Correlation analysis (**F**) Correlation analysis between ACCPA and GUDCA levels: The ACCPA concentration negatively correlates with GUDCA with r = -0.5882 significantly. (**G**) The graph shows a negative correlation between GUDCA and DAS28-ESR score with r = -0.5749 in RA. Log2FC; log2 fold change, RA; rheumatoid arthritis, HC; healthy control, ACCPA; anti-citrullinated protein/peptide antibody, DAS28-ESR; Disease Activity Score 28-joint count- erythrocyte sedimentation rate

10 min. The densitometric analysis demonstrated a significantly decreased expression of NFκB (p65) ($p < 0.0164$) at 50μM of GUDCA concentration (Fig. 4B). The protein ($p < 0.0159$) expression of the IGF1 was upregulated (Fig. 4C), whereas the TTR level was downregulated ($p < 0.0193$) (Fig. 4D) by GUDCA induction at 50μM as compared to the control + TNFα. Subsequently, GUDCA treatment at 50μM concentration also showed a significant rise in the mRNA expression of IGF1 ($p < 0.0152$) (Fig. 4E) and a decrease in the mRNA expression of TTR ($p < 0.0027$) (Fig. 4F), IL-6 ($p < 0.0001$) (Fig. 4G), IL1β($p < 0.0118$) (Fig. 4H) and NFκB (p65) ($p < 0.0005$)

Table 2 List of significantly 29 upregulated and 23 downregulated differentially regulated proteins with Fold change and p-value

S.No	Protein	fold change	pvalue
1	Apolipoprotein C-I	62.40570335	0.007758662
2	Alpha-1-acid glycoprotein 1	16.7214335	0.00553161
3	Apolipoprotein C-III	9.850330468	1.25567E-06
4	Complement C4-A	8.302636966	0.002453229
5	Complement C4-B	8.023461599	0.000342575
6	Inter-alpha-trypsin inhibitor heavy chain H4	6.888252287	0.008452104
7	Hemopexin	5.921200271	0.010553529
8	Apolipoprotein A-I	4.808899273	0.00343186
9	Complement C1r subcomponent	4.738477563	0.018669551
10	Ig kappa chain V-I region EU	3.814368748	0.012133217
11	Angiotensinogen	3.583448101	0.008352337
12	Fibrinogen alpha chain	3.47708266	0.026347715
13	Complement C1q subcomponent subunit B	3.417463883	0.011119125
14	CD5 antigen-like	3.100496169	0.033706855
15	Hemoglobin subunit beta	2.657607982	0.007641719
16	Alpha-1-antitrypsin	2.536239559	0.013834211
17	Serum paraoxonase/arylesterase 1	2.285135829	0.035481367
18	Cartilage acidic protein 1	2.195281727	0.027063039
19	Clusterin	2.19471443	0.001684064
20	Dipeptidyl peptidase 4	2.11232999	0.016101272
21	Inter-alpha-trypsin inhibitor heavy chain H3	2.056770621	0.012397008
22	Serum amyloid A-4 protein	2.055016548	0.043047554
23	Transthyretin	1.897613179	0.048515129
24	Protein AMBP	1.885350481	0.016866094
25	Alpha-1-antichymotrypsin	1.83019933	0.035537119
26	Complement component C9	1.814339568	0.049834854
27	Leucine-rich alpha-2-glycoprotein	1.717204308	0.03938007
28	Ceruloplasmin	1.694083887	0.003258636
29	Thyroxine-binding globulin	1.659605788	0.045789643
30	L-selectin	0.507441747	0.038241024
31	Biotinidase	0.48889523	0.047922207
32	N-acetylmuramoyl-L-alanine amidase	0.465354202	0.004123615
33	Ig heavy chain V-III region ZAP	0.454522581	0.047582617
34	Histidine-rich glycoprotein	0.45196089	0.013256396
35	Insulin-like growth factor I	0.42957407	0.016637558
36	72 kDa type IV collagenase	0.427441571	0.058048635
37	Afamin	0.427009471	0.025087744
38	Ig heavy chain V-III region LAY	0.409704949	0.023839039
39	Complement component C8 gamma chain	0.394727685	0.006947765
40	Eukaryotic initiation factor 4 A-II	0.383639153	0.039364223
41	Heparin cofactor 2	0.35791362	0.001140975
42	Coagulation factor XII	0.35345247	0.039938135
43	C-reactive protein	0.299366867	0.006885079
44	Complement component C8 alpha chain	0.282144005	0.004202023
45	Selenoprotein P	0.279631127	0.003575084
46	ATP-binding cassette sub-family F member 1	0.220376839	0.02683651
47	Lumican	0.210071273	0.022956686
48	Monocyte differentiation antigen CD14	0.200887807	0.002936902
49	Fibulin-1	0.190617853	0.005701437
50	Coagulation factor XIII A chain	0.089036558	0.039629791
51	Fetuin-B	0.062425822	0.006111321
52	C4b-binding protein beta chain	0.052992974	0.000368021

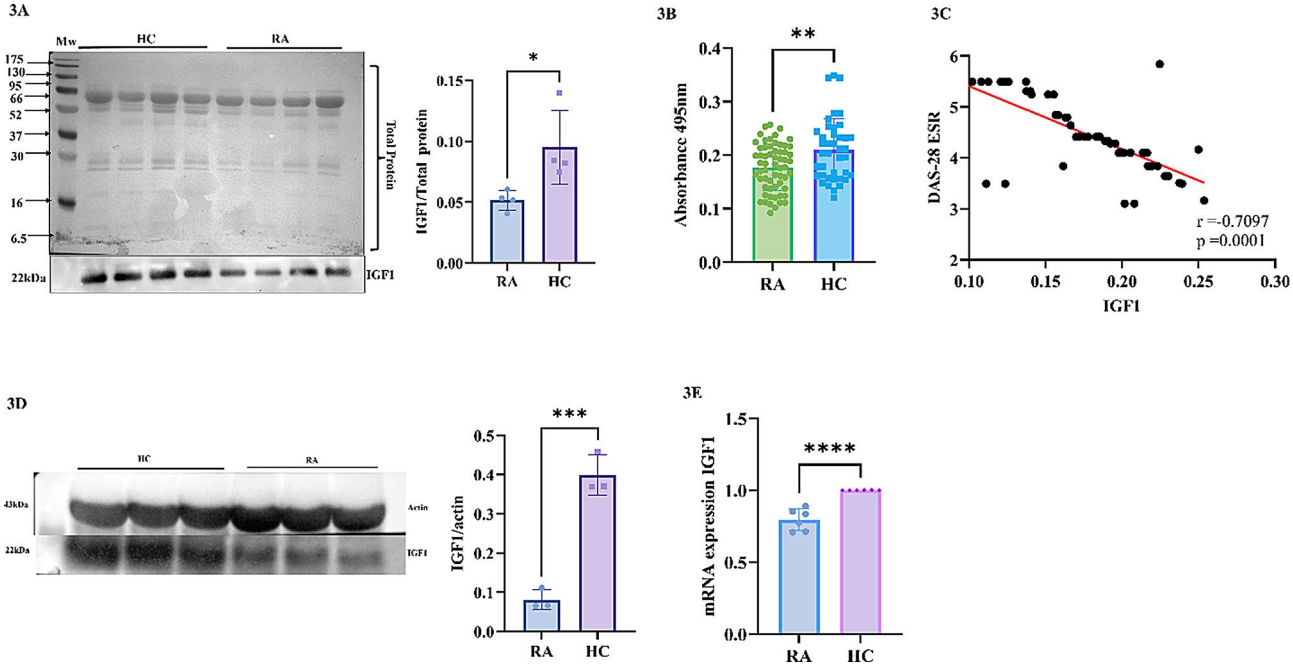

Fig. 3 (**A**) Western blot analysis of IGF1 in RA representing the level of IGF1 in RA ($n=40$) pooled plasma compared to HC ($n=40$) ($p<0.0349$) with 1.6-fold downregulated expression. (**B**) The expression of IGF1 by ELISA in RA Plasma ($n=60$) and control ($n=40$) indicated a significantly low-level expression with a 1.2-fold ($p<0.0011$) compared to HC. (**C**) Correlation analysis between IGF1 and DAS28-ESR score shows a significant negative correlation with r = -0.7097 in RA patients. (**D**) Western blot analysis of IGF1 in PBMCs representing the significantly downregulated expression of IGF1 ($p<0.0007$) in RA PBMCs compared to HC ($n=6$ each) (**E**) Significantly downregulated gene expression of IGF1 ($p<0.0001$) in RA PBMCs compared to HC ($n=6$ each) by qRT-PCR. The statistical significance was determined by Student's t-test, $p<0.05$. RA; rheumatoid arthritis, HC; healthy control, Mw; molecular weight, IGF1;insulin-like growth factor-1; ELISA; Enzyme-Linked ImmunoSorbent Assay, PBMC; Peripheral blood mononuclear cells, qRT-PCR; Real-Time Quantitative Reverse Transcription PCR, * = $P\leq0.05$, ** = $P\leq0.01$, *** = $P\leq0.001$, ****=$P\leq0.0001$

(Fig. 4I) compared to control+TNFα. Thus, GUDCA pre-treatment significantly decreased the inflammation level compared to the control, concluding that GUDCA metabolite possesses anti-inflammatory properties.

GUDCA inhibits cell migration and invasion in synovial fibroblasts

The wound healing assay was carried out to determine the effect of GUDCA on cell migration and invasion capability. The results indicated a decrease in the migration of cells when treated with GUDCA(50μM) at 48 h compared to the untreated cells (C) at the same time points, indicating that GUDCA can inhibit cell migration and invasion of cells. The gaps marked in the untreated control cells (C) and TNF-α induced SW982 cells (control+TNFα) were almost filled with the migration of cells, while the cell's migratory ability in the GUDCA(50μM)-treated group was observed to be significantly less. The inhibition of cell migration was 41.0% in TNF-α treated cells, 66.9% in control cells, and 85.9% after treatment with GUDCA (50μM) at 48 h, indicating that GUDCA has the potential of an antiproliferative agent since it inhibits cell migration under inflammatory conditions. (Fig. 5A).

Reactive oxygen scavenging (ROS) ability of GUDCA

Oxidative stress was measured by estimating the total cellular ROS in GUDCA (50μM) pretreated cells (SW982) with/without TNF-α for 24 h. Fluorescence signals of cells were measured by DCFHDA dye and showed highly induced intracellular ROS production in TNF-α induced cells compared to untreated control cells. GUDCA treatment, therefore, significantly ($p\leq0.0004$) inhibited the intracellular ROS production in TNF-α induced SW982 cells (Fig. 5B).

CIA-Rat model establishment, amelioration of clinical severity, by GUDCA treatment

The CIA rat model is widely used to mimic the RA condition [31] and the effect of GUDCA was investigated in the model. Images of rat paws taken on the 28th day of all groups Group 1 (HC), Group 2 (CIA), Group 3 (CIA+VC), and Group 4 (CIA+GUDCA) before scarification are shown (Fig. 6A). We observed that Group 4 showed less redness and swelling compared to Groups 2 and 3. The development of arthritis was quantified by measuring the paw volume using plethysmometer twice weekly to confirm the onset of the disease. After day 14, the average paw volume decreased in Groups 4, whereas paw volume increased in Groups 2 and 3 (Fig. 6B).

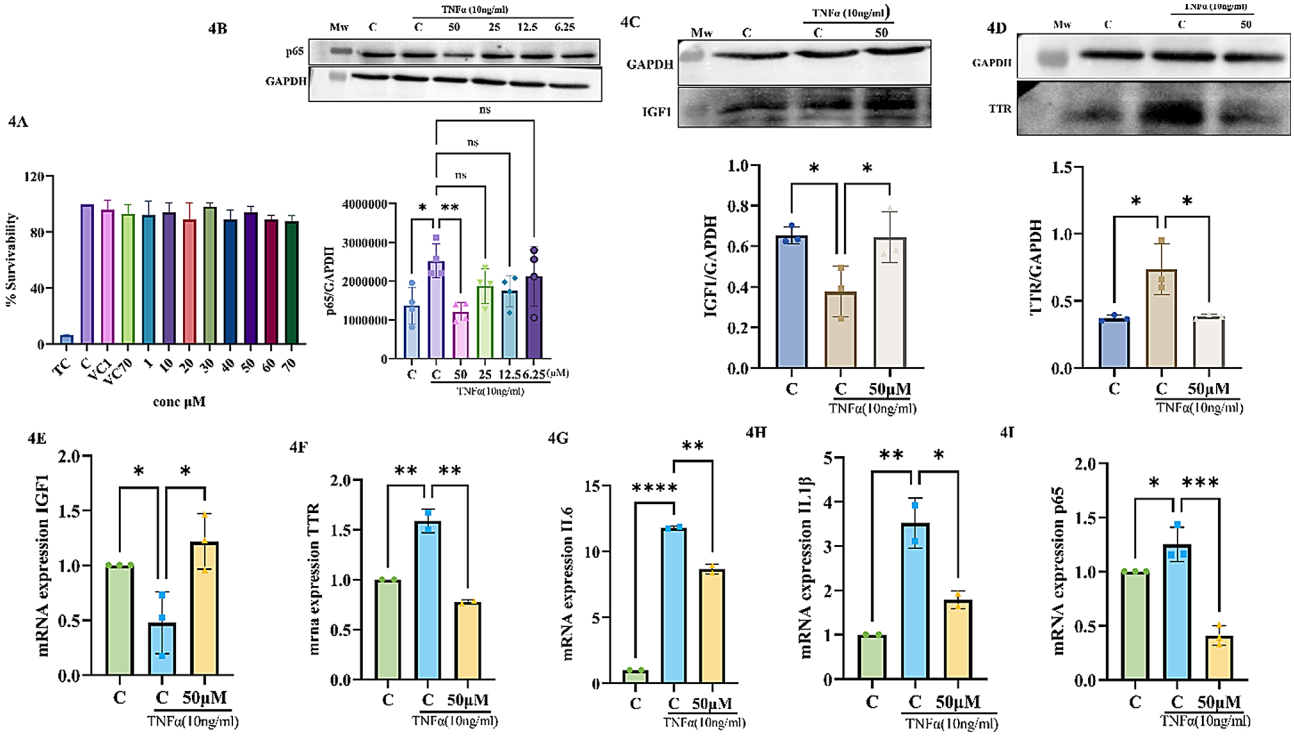

Fig. 4 (**A**) The cell viability test by the MTT assay representing the cell viability results of SW982 cells treated with GUDCA (1–70 µM/ml) for 24 h (**B**) Western Blot analysis- The expression level of p65, pre-treated with serial dilutions of GUDCA (50µM to 6.25µM) with or without TNF-α (10 ng/ml) for 10 min was observed significantly ($p < 0.0164$) downregulated at 50µM of GUDCA in SW982 cells. (**C**) Significantly ($p < 0.0159$) upregulated expression of IGF1 analyzed by Western Blot in SW982 cells, pre-treated with 50µM GUDCA for 24 h with or without TNF-α (10ng/ml) induction for 10 min (**D**) Significantly ($p < 0.0193$) downregulated expression of TTR analyzed by Western Blot in SW982 cells, pre-treated with 50µM GUDCA for 24 h with or without TNF-α (10 ng/ml) induction for 10 min. Densitometric analysis of GUDCA treatments normalized by GAPDH. (**E**) mRNA expression analysis of IGF1 by qRT-PCR in SW982 cells pretreated with GUDCA (50µM) for 24 h and induction of TNF-α (10 ng/ml) for 1 h. The mRNA expression of IGF1 was observed significantly ($p < 0.0152$) upregulated (**F**) mRNA expression of TTR was observed significantly ($p < 0.0027$) downregulated (**G**) IL6 gene expression significantly ($p < 0.0001$) downregulated (**H**) IL1β gene expression significantly ($p < 0.0118$) downregulated (**I**) p65 gene expression significantly ($p < 0.0005$) downregulated compared to control with TNF-α. The data normalized with GAPDH as an internal loading control, and the values presented as the mean ± SEM ($n = 3$). MTT; 3-(4,5-Dimethylthiazol-2-yl)-2,5-diphenyltetrazolium bromide, GUDCA; Glycoursodeoxycholic acid, TTR; Transthyretin, SEM; Standard error of the mean, C; control cells without TNF-α and GUDCA, Mw; molecular weight, tc; toxic control, vc; vehicle control, IGF1;insulin like growth factor-1, IL1β; interleukinβ, IL6; interleukin 6, GAPDH; Glyceraldehyde 3-phosphate dehydrogenase, ns; non-significant, * = $P \leq 0.05$, ** = $P \leq 0.01$, *** = $P \leq 0.001$, ****=$P \leq 0.0001$

CIA-induced arthritis was determined to progress successfully by measuring arthritis index (AI%) between the groups. (Fig. 6C). AI was more in group 2 and 3, that was decreased in group 4. The increased presence of autoreactive B cells in RA leads to elevated production of immunoglobulins and enlargement of the spleen. In CIA rats, the liver and spleen are susceptible to chronic inflammation that can be measured as splenic and liver index. In Group 2, the splenic index (Fig. 6D) and liver index (Fig. 6E) increased compared to normal rats, which was found to be normalized by GUDCA, exhibiting protective effects. Pro-inflammatory cytokine levels were also quantitively measured in the rat plasma of all groups. Downregulation of pro-inflammatory cytokines (TNFα, IL-1β, IL-6) were also revealed in rat plasma in Groups 4 compared to Groups 2 and 3 (Fig. 6F).

GUDCA ameliorated inflammatory stress of synovium

To further validate the anti-inflammatory activity of GUDCA, histological tests were performed on rat synovium by H&E staining (Fig. 6G). The pink color represents cytoplasm, which correlates with the synovium's inflammation. The purple color represents the number of nuclei present, used to determine the number of cells infiltrated into the given region and to quantify inflammation [31]. The H&E scan analysis revealed that the group injected with GUDCA (Group 4) exhibited much less cell infiltration compared to Groups 3 and 2 (Fig. 6H). This histological examination supports the idea that Group 4 significantly reduces inflammation in the CIA rats.

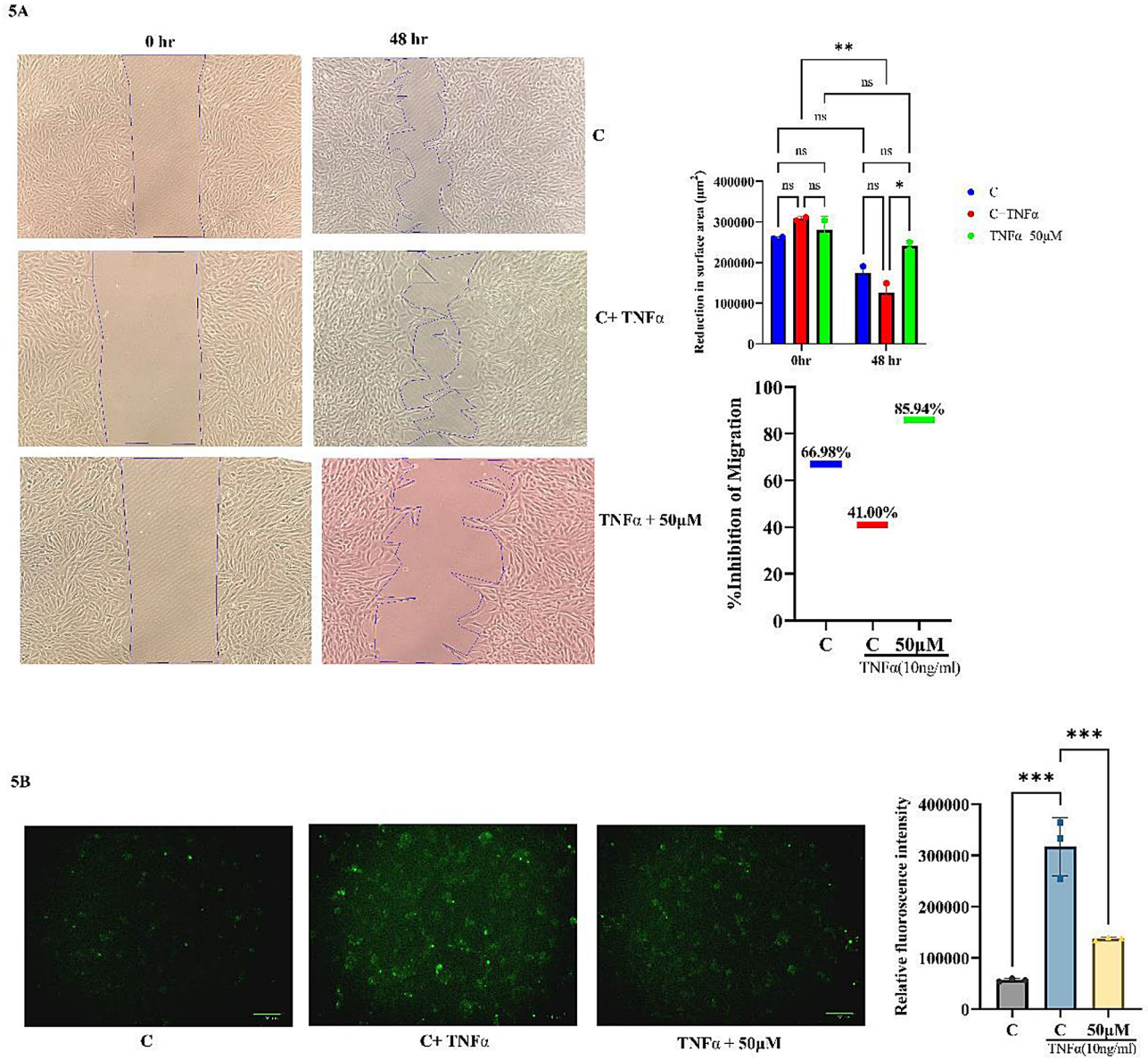

Fig. 5 (**A**) Scratch assay: Migration ability of SW982 cells by scratch assay after stimulation with GUDCA 50μM for 24 h with or without TNF-α (10 ng/ml). The results showed that the %inhibition of migration in control was 66%, in TNF-α treated cells 41%, and GUDCA treated cells 85% at 48 h compared to 0 h. ****$p \leq 0.0001$. (**B**) Totalcellular ROS was analyzed after GUDCA (50μM) pretreatment for 24 h with/without TNF-α (10ng/ml) using DCFHDA probe. GUDCA treatment inhibited ROS production observed by fluorescence intensity significantly ($p < 0.0004$) compared to TNF-α induced and control cells (**C**). Error bars represent the mean ± SEM from three independent experiments. C; control cells without TNF-α and GUDCA, GUDCA; Glycoursodeoxycholic acid, ROS; reactive oxygen species, DCFHDA; dichlorodihydrofluorescein diacetate, ANOVA; Analysis of Variance, SEM; Standard error of the mean, ns; nonsignificant, * = $P \leq 0.05$, ** = $P \leq 0.01$, *** = $P \leq 0.001$, ****=$P \leq 0.0001$

Effect of GUDCA on differential regulation of TTR and IGF1 in CIA-rat plasma

The impact of GUDCA on the differential regulation of proteins was assessed through WB analysis in CIA rat plasma. The findings indicated that GUDCA was able to decrease the expression of TTR and increase the expression of IGF1 in Group 4. Densitometric analysis showed a significant increase in the expression of IGF1 (p=0.0101; Fig. 6I) and a decrease in the expression of TTR (p=0.0013; Fig. 6J). Similar results were observed in the synovium of CIA rats using ELISA. The ELISA results demonstrated a significant reduction in TTR levels (Fig. 6K) and an increase in the expression of IGF1 in Group 4 compared to CIA (Fig. 6L). Therefore, we may conclude that GUDCA may have the ability to regulate the expression of these proteins.

The increased levels of TTR and decreased levels of IGF1 are linked to inflammatory markers (IL-6, IL-1β) that contribute to the progression of RA. This data was

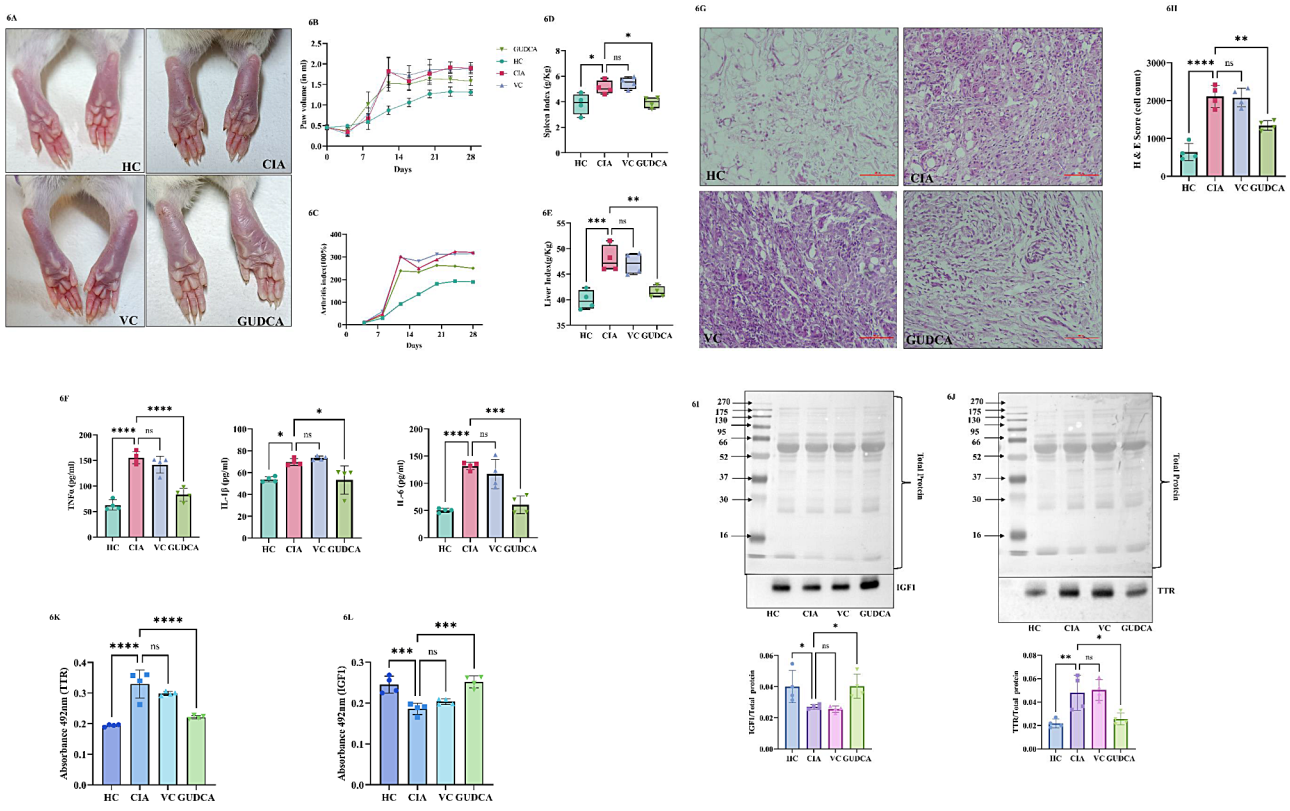

Fig. 6 The effect of GUDCA on collagen-induced arthritis rat model: (**A**) Visual representative of hind paw image of the rats from each group, where edema and redness were reduced in Groups 4 compared to Groups 2 and 3. (**B**) Graphical representation of measured paw volume from day 0 to day 28, depicting the changes in paw volume in Group 4 compared to Groups 2 and 3. (**C**) Shows the attenuation of clinical Arthritis index (%) was reduced upon treatment of GUDCA to the CIA group compared to control and indicates a significant difference between the groups. (**D**) Effects of GUDCA on the spleen index of CIA mice on the day of scarification. The weight of spleens in CIA mice was significantly larger than those of normal mice represented as spleen weight/ body weight (g/Kg). Similarly, (**E**) Liver index was calculated. (**F**) Validation of pro-inflammatory parameter: the levels of the proinflammatory cytokine were measured by quantitative ELISA analysis in rat plasma in Groups 1 to 4, showing the downregulation of TNF α, IL-1β, and IL-6 levels in Groups 4 compared to Groups 2 and 3 (**G**) The H&E staining shows decreased cell inflammation (purple color) in Group 4 compared to Groups 2 and 3 (**H**) The analysis of cell infiltration in the synovium was measured as cell count by Image J and represented as H&E score found to be downregulated in groups 4 compared to groups 2 and 3. Western Blot analysis of TTR and IGF1 in plasma of CIA-RAT Model (**I**) The band intensities of the CIA group show a significantly decreased level of IGF1($p=0.05$) in plasma compared to the control; the treatment with GUDCA effectively increased the expression level in plasma of CIA arthritis model of RA. (**J**) Similarly, a significantly increased level of TTR ($p=0.05$) shows expression in plasma, and the treatment with GUDCA effectively decreased the expression normalized by total protein. Indirect ELISA of Synovium (**K**) Significantly reduced level of TTR was found in the GUDCA treated group compared to CIA and VC group (**L**) Increased IGF1 expression after GUDCA treatment in rats compared to the CIA group. (Group1: Healthy or HC, Group2: CIA, Group3: CIA + VC, Group4: CIA + GUDCA, * = $P \leq 0.05$, ** = $P \leq 0.01$, *** = $P \leq 0.001$)

validated for the first time in synovial fibroblast cells, showing that treatment with GUDCA in both the synovial fibroblast cells and the CIA rat model reduces the exacerbation of disease severity.

Discussion

RA holds a crucial social, economic, and physiological burden on affected individuals. It dramatically impacts people's bone health, and deformity leads to disability [1, 32]. Prevalent systemic inflammation in RA is mediated by pro-inflammatory cytokines that affect different cellular metabolism [5, 8].

We utilized metabolomics and proteomics techniques, and revealed 82 metabolites and 231 differentially regulated proteins in RA with high confidence. Differential molecular patterns of metabolites and proteins were integrated using biological pathways analysis [33] and joint pathway analysis [34] and revealed "Porphyrin metabolism" as a prominent pathway associated with RA. This pathway was associated with the metabolites Glycocholic acid, Glycodeoxycholic acid, and Glycoursodeoxycholic acid (GUDCA) (bile acids conjugates).

The report indicates that Glycocholic acid and Glycodeoxycholic acid are vital in regulating bile acid synthesis, depending on the availability of cholesterol substrate, and significantly reduce HMG-CoA reductase activity [35, 36]. GUDCA is obtained from the acyl glycine conjugate of ursodeoxycholic acid [37, 38] which is reported to have a neuroprotective and anti-inflammatory agent [39]. Ursodeoxycholic acid can dissolve cholesterol gallstones

and treat cholestatic liver disorders, atherosclerosis, steatosis, and liver fibrosis [40, 41]. It has been proven to effectively prevent pain and cartilage degeneration in cases of osteoarthritis (OA). Its chondroprotective properties work by effectively suppressing oxidative damage and inhibiting catabolic factors that are known to contribute to the pathogenesis of cartilage damage in OA [40–43].

In our study on RA, we found that the level of GUDCA showed a negative correlation with disease severity as assessed by ACCPA levels and DAS28-ESR activity score. This led us to suspect that GUDCA might hold promise as a new treatment for RA. As a result, we have chosen to further analyze the therapeutic potential of GUDCA.

To explore the potential targets of GUDCA, PharmMapper analysis of GUDCA and comparative study with differential proteomics profile was attempted and revealed that IGF1 and TTR can be the appropriate targets of GUDCA. IGF1 has a link with inflammation and immuno-metabolism and is associated with bone and cartilage differentiation [44]. Its bioactivity is controlled by six IGF-binding proteins (IGFBP-1 to IGFBP-6). Low expression of IGF1 in the sera of RA patients increased with disease activity [45] supported by our SWATH data. Increased levels of IGF1 promote articular cartilage regeneration after injury [46]. Thus, the effect of GUDCA on the expression of IGF1 and its association in synovial fibroblast cells with inflammation related to RA pathogenesis was examined.

Significantly decreased levels of IGF1 in RA plasma and PBMCs suggested its low availability in RA (Fig. 3A and D). The levels of IGF1 were found to have a negative correlation with the DAS28-ESR score (Fig. 3C). The report shows that differentiation of bone and cartilage tissue is hampered due to less availability of IGF1 in RA [46]. IGF1 is thus unable to participate in regulating immunity and inflammation, and that promotes the disease conditions.

We also selected a significantly upregulated protein, TTR, from SWATH data, a pre-albumin secretory protein that transports retinol and thyroxin (T4). In our previous study, we discovered that the increased rate of TTR glycation, along with its binding with RAGE, serves as a trigger for inflammatory pathways through the activation of NF-kB [20]. To confirm the therapeutic ability of GUDCA, the expression of IGF1 and TTR by in vitro studies was analyzed. Expression levels of p65 were reduced in the presence of GUDCA at both protein and mRNA levels. The simultaneous observation of increased IGF1 levels and decreased TTR levels after GUDCA treatment suggests that GUDCA actively regulates these levels, thus playing a significant role in inflammation. Also, GUDCA has been found to have an anti-proliferative and antioxidative effect on synovial fibroblast cells (Fig. 5A, B). Further, our findings were validated in the CIA rat model. GUDCA helped to improve disease symptoms in CIA rats by significantly reducing paw volume and arthritis index. There was also a significant decrease in immune cell infiltration in the GUDCA treated group compared to the CIA group, as indicated by the H&E score (Fig. 6G). Additionally, analysis of CIA rat plasma showed that the levels of the proteins (TTR and IGF1) were altered by GUDCA concentration, indicated reduced pathogenesis of RA.

Conclusion

Our study demonstrated that GUDCA may have a protective effect on the disease development of RA pathogenesis. The untargeted metabolomics by HPLC-MS/MS revealed metabolites and DEPs of RA, and laid the foundation for monitoring disease development based on the interplay of both biomolecules (metabolite and protein). The explanation of metabolic pathways in chronic inflammatory circumstances such as RA provided new insight into disease development. It offered a hopeful sign for the specific biomolecular marker identification for RA. Further, the mechanistic evaluation of GUDCA at the cellular level needs to be explored, and its therapeutic impact must be validated. Additionally, rigorous clinical studies are essential to validate the therapeutic impact of GUDCA. These studies should encompass diverse patient populations, dosage regimens, and treatment durations to accurately assess its efficacy and safety profile. These meticulous steps are paramount for gaining a profound understanding of the potential benefits of this metabolite and its implications for human health.

Limitations

The patients pooled in this study have established RA and are all undergoing pharmacological treatment, including glucocorticoids. Consequently, the potential influence of these medications on the differential metabolites cannot be entirely excluded. Therefore, validation in an untreated RA cohort would be desirable. However, it is very difficult to collect such samples. Moreover, it has been elucidated that GUDCA may be associated with the regulation of pro-inflammatory cytokines, potentially serving as a modulator of RA disease activity. Further, investigation into the intracellular molecular mechanisms revealing the inflammatory control, including direct associations with IGF1 and TTR, is necessary for clear understanding.

Abbreviations

RA	Rheumatoid arthritis
HC	Healthy control
DEPs	Differentially expressed proteins
CIA	Collagen Induced Arthritis
RIPA	Radioimmunoprecipitation assay buffer
DMEM	Dulbecco's Modified Eagle Medium

GUDCA	Glycoursodeoxycholic acid
ACR	American College of Rheumatology
EULAR	European League Against Rheumatism
GAPDH	Glyceraldehyde-3-phosphate dehydrogenase
ROS	Reactive oxygen species
DCFHDA	Dichlorodihydrofluorescein diacetate
HPLC-MS HPLC/LC-MS/MS	High Performance Liquid Chromatography-Mass Spectrometry
SWATH-MS	Sequential Window Acquisition of all Theoretical Mass Spectra
EDTA	Ethylenediamine tetra acetic acid
LC-MS/MS	Liquid chromatography–tandem mass spectrometry
HILIC	Hydrophilic interaction liquid chromatography
NIST	National Institute of Standards and Technology
BCA	Bicinchoninic Acid
GDA	Gene Disease association
SDS-PAGE	Sodium dodecyl-sulfate polyacrylamide gel electrophoresis
PCR	Polymerase chain reaction
MTT	3-(4,5-Dimethylthiazol-2-yl)-2,5-diphenyltetrazolium bromide
ER	Endoplasmic reticulum
HFD	High fat diet
IGF1	insulin-like growth factor-1
RAGE	Receptor for Advanced Glycation Endproducts
ACCPA	Anti-citrullinated protein/peptide antibody
DAS28-ESR scores	disease activity score - erythrocyte sedimentation rate
DCFH-DA	Dichloro-dihydro-fluorescein diacetate
PBS	Phosphate-buffered saline
ICMR	Indian Council of Medical Research
OPLS-DA	Projections to Latent Structures Discriminant Analysis
PCA	Principal component analysis
VIP	Variable importance projection
SHBG	Sex hormone-binding globulin
ECL	Electrochemiluminescence
HRP	Horseradish peroxidase
HMG-CoA	Hydroxymethylglutaryl-CoA

Supplementary Information

The online version contains supplementary material available at https://doi.org/10.1186/s13075-024-03429-z.

Supplementary Material 1

Supplementary Material 2

Supplementary Material 3

Supplementary Material 4

Supplementary Material 5

Supplementary Material 6

Acknowledgements

We acknowledge the Council of Scientific and Industrial Research (CSIR), and DST- Science & Engineering research board (SERB), Government of India, New Delhi, India, for providing financial support. Lovely Joshi, Mohd Saquib, Ashish and Debolina received fellowship support from CSIR. Prachi Agnihotri, Swati Malik received a fellowship from DST. Mr. Praveen for mass spectrometer data acquisition and Mr. Pankaj Yadav for transporting biological samples from the hospital to the lab. We also thank CSIR-Institute of Genomics and Integrative Biology, Delhi, India to provide the research platform, AcSIR for academic support, and the Department of Rheumatology, All India Institute of Medical Sciences (AIIMS), New Delhi, India for providing patient's sample.

Author contributions

All authors have made substantial contributions to data analysis and took part in drafting the article or revising it critically for important intellectual content and agreed to submit it to the current journal. Prachi and Dr Sagarika Biswas made substantial contributions to the conception, design, drafting, acquisition of data, or analysis and interpretation of data. Swati, Lovely, Saquib, Ashish and Debolina contributed in drafting, data analysis, and sample handling. Dr Uma Kumar provided the biological samples. Dr Sagarika Biswas agreed to submit to the current journal, gave final approval for the version to be published, and agreed to be accountable for all aspects of the work.

Funding

We would like to acknowledge the Department of Science and Technology (DST), Science & Engineering Research Board (SERB) CRG/2019/006398, New Delhi, India for financial support.

Data availability

For all original data and protocol, please contact Dr Sagarika Biswas (Sagarika.biswas@igib.res.in).

Declarations

Ethics approval

The study protocol was ethically approved by AIIMS, New Delhi, India (Reg No IEC-37/07.02.2020, RP-15/2020) and the study protocols complied with the Declaration of Helsinki. The work design was approved by the Institute's Animal Ethical Committee (IGIB/IAEC/3/3/Mar 2023).

Consent for publication

All the authors have agreed that the study should be submitted to Journal.

Conflict of interests

The authors declare no conflict of interests.

Author details

[1]Integrative and Functional Biology Department, Council of Scientific & Industrial Research (CSIR)-Institute of Genomics and Integrative Biology, Mall Road, Delhi University Campus, Delhi 110007, India
[2]Academy of Scientific and Innovative Research (AcSIR), Ghaziabad 201002, India
[3]All India Institute of Medical Sciences, Ansari Nagar, New Delhi 110029, India

Received: 8 August 2024 / Accepted: 3 November 2024
Published online: 23 December 2024

References

1. Guo Q, Wang Y, Xu D, Nossent J, Pavlos NJ, Xu J. Rheumatoid arthritis: pathological mechanisms and modern pharmacologic therapies. Bone Res. 2018;6. https://pmc.ncbi.nlm.nih.gov/articles/PMC5920070/
2. Scherer HU, Häupl T, Burmester GR. The etiology of rheumatoid arthritis. J Autoimmun. 2020;110:102400.
3. Oliver AM. St. Clair EW. Rheumatoid arthritis C. treatment and assessments. Primer on the Rheumatic Diseases: Thirteenth Edition. 2008;133–41. https://link.springer.com/chapter/10.1007/978-0-387-68566-3_6
4. Chen J, Li S, Zhu J, Su W, Jian C, Zhang J, et al. Multi-omics profiling reveals potential alterations in rheumatoid arthritis with different disease activity levels. Arthritis Res Ther. 2023;25. Available from: https://pmc.ncbi.nlm.nih.gov/articles/PMC10155393/.
5. Yap HY, Tee SZY, Wong MMT, Chow SK, Peh SC, Teow SY. Pathogenic role of immune cells in rheumatoid arthritis: implications in clinical treatment and biomarker development. Cells. 2018;7. https://pmc.ncbi.nlm.nih.gov/articles/PMC6211121/
6. Tounta V, Liu Y, Cheyne A, Larrouy-Maumus G. Metabolomics in infectious diseases and drug discovery. Mol Omics. 2021;17:376. https://pmc.ncbi.nlm.nih.gov/articles/PMC8202295/
7. Rinschen MM, Ivanisevic J, Giera M, Siuzdak G. Identification of bioactive metabolites using activity metabolomics. Nat Rev Mol Cell Biol. 2019;20:353. https://pmc.ncbi.nlm.nih.gov/articles/PMC6613555/
8. Wishart DS. Metabolomics for investigating physiological and pathophysiological processes. Physiol Rev. 2019;99:1819–75. https://doi.org/10.1152/physrev.00035.2018

9. van der Knaap JA, Verrijzer CP. Undercover: gene control by metabolites and metabolic enzymes. Genes Dev. 2016;30:2345. Available from: https://pmc.ncbi.nlm.nih.gov/articles/PMC5131776/.
10. Krijgsveld J, Neagu A-N, Whitham D, Seymour L, Haaker N, Pelkey I, et al Proteomics-Based Identification of Dysregulated Proteins and Biomarker Discovery in Invasive Ductal Carcinoma, the Most Common Breast Cancer Subtype. Proteomes. 2023;11:13. https://www.mdpi.com/2227-7382/11/2/13/htm
11. Hua C, Daien CI, Combe B, Landewe R. Diagnosis, prognosis and classification of early arthritis: results of a systematic review informing the 2016 update of the EULAR recommendations for the management of early arthritis. RMD Open. 2017;3. https://pubmed.ncbi.nlm.nih.gov/28155923/
12. Biswas S, Sharma S, Saroha A, Bhakuni DS, Malhotra R, Zahur M, et al. Identification of novel autoantigen in the synovial fluid of rheumatoid arthritis patients using an immunoproteomics approach. PLoS One. 2013;8:e56246. https://journals.plos.org/plosone/article?id=10.1371/journal.pone.0056246
13. Shan M, Liu H, Hao Y, Song K, Meng T, Feng C, et al. Metabolomic profiling reveals that 5-Hydroxylysine and 1-Methylnicotinamide are metabolic indicators of Keloid Severity. Front Genet. 2022;12:804248.
14. Basak T, Varshney S, Hamid Z, Ghosh S, Seth S, Sengupta S. Identification of metabolic markers in coronary artery disease using an untargeted LC-MS based metabolomic approach. J Proteomics. 2015;127:169–77. https://pubmed.ncbi.nlm.nih.gov/25790721/
15. Monu, Kharb R, Sharma A, Chaddar MK, Yadav R, Agnihotri P, et al. Plasma proteome profiling of coronary artery disease patients: downregulation of transthyretin-an important event. Mediators Inflamm. 2020;2020. https://pubmed.ncbi.nlm.nih.gov/33299376/
16. An R, Yu H, Wang Y, Lu J, Gao Y, Xie X, et al. Integrative analysis of plasma metabolomics and proteomics reveals the metabolic landscape of breast cancer. Cancer Metab. 2022;10. Available from: https://pmc.ncbi.nlm.nih.gov/articles/PMC9382832/.
17. Núñez S, Venhorst J, Kruse CG. Target-drug interactions: first principles and their application to drug discovery. Drug Discov Today. 2012;17:10–22.
18. Wang JH, Byun J, Pennathur S. Analytical approaches to metabolomics and applications to systems biology. Semin Nephrol. 2010;30:500–11. https://pubmed.ncbi.nlm.nih.gov/21044761/
19. Liu X, Ouyang S, Yu B, Liu Y, Huang K, Gong J, et al. PharmMapper server: a web server for potential drug target identification using pharmacophore mapping approach. Nucleic Acids Res. 2010;38. https://pubmed.ncbi.nlm.nih.gov/20430828/
20. Monu, Agnihotri P, Saquib M, Sarkar A, Chakraborty D, Kumar U, et al. Transthyretin and receptor for advanced glycation end product's differential levels associated with the pathogenesis of rheumatoid arthritis. J Inflamm Res. 2021;14:5581. https://pmc.ncbi.nlm.nih.gov/articles/PMC8560178/.
21. DAS 28 -. Disease activity score calculator for rheumatoid arthritis. https://www.4s -dawn.com/D AS28/ Accessed 15 Jul 2024.
22. Rakhecha B, Agnihotri P, Dakal TC, Saquib M, Monu, Biswas S. Anti-inflammatory activity of nicotine isolated from Brassica oleracea in rheumatoid arthritis. Biosci Rep. 2022;42. https://pubmed.ncbi.nlm.nih.gov/35289351/
23. Khansai M, Phitak T, Klangjorhor J, Udomrak S, Fanhchaksai K, Pothacharoen P, et al. Effects of sesamin on primary human synovial fibroblasts and SW982 cell line induced by tumor necrosis factor-alpha as a synovitis-like model. BMC Complement Altern Med. 2017;17. https://pubmed.ncbi.nlm.nih.gov/29237438/
24. Sarkar A, Chakraborty D, Kumar V, Malhotra R, Biswas S. Upregulation of leucine-rich alpha-2 glycoprotein: a key regulator of inflammation and joint fibrosis in patients with severe knee osteoarthritis. Front Immunol. 2022;13:1028994.
25. Bendele A, Mccomb J, Gould T, Mcabee T, Sennello G, Chlipala E, et al. Animal models of arthritis: relevance to human disease. Toxicol Pathol. 1999;27:134–42. https://pubmed.ncbi.nlm.nih.gov/10367688/
26. Bai L, Bai Y, Yang Y, Zhang W, Huang L, Ma R, et al. Baicalin alleviates collagen-induced arthritis and suppresses TLR2/MYD88/NF-κB p65 signaling in rats and HFLS-RAs. Mol Med Rep. 2020;22:2833. https://pmc.ncbi.nlm.nih.gov/articles/PMC7453616/.
27. Wang QS, Xu BX, Fan KJ, Li YW, Wu J, Wang TY. Dexamethasone-loaded thermosensitive hydrogel suppresses inflammation and pain in collagen-induced arthritis rats. Drug Des Devel Ther. 2020;14:4101. https://pmc.ncbi.nlm.nih.gov/articles/PMC7547127/.
28. De S, Manna A, Kundu S, De Sarkar S, Chatterjee U, Sen T, et al. Allylpyrocatechol attenuates collagen-induced arthritis via attenuation of oxidative stress secondary to modulation of the MAPK, JAK/STAT, and Nrf2/HO-1 pathways. J Pharmacol Exp Ther. 2017;360:249–59. https://jpet.aspetjournals.org/content/360/2/249
29. Monu, Agnihotri P, Saquib M, Biswas S. Targeting TNF-α-induced expression of TTR and RAGE in rheumatoid arthritis: apigenin's mediated therapeutic approach. Cytokine. 2024;179:156616.
30. Kurowska W, Kuca-Warnawin EH, Radzikowska A, Maslinski W. The role of anti-citrullinated protein antibodies (ACPA) in the pathogenesis of rheumatoid arthritis. Cent Eur J Immunol. 2017;42:390. https://pmc.ncbi.nlm.nih.gov/articles/PMC5820977/.
31. Bai L, Bai Y, Yang Y, Zhang W, Huang L, Ma R, et al. Baicalin alleviates collagen-induced arthritis and suppresses TLR2/MYD88/NF-κB p65 signaling in rats and HFLS-RAs. Mol Med Rep. 2020;22:2833. https://pmc.ncbi.nlm.nih.gov/articles/PMC7453616/.
32. Smolen JS, Aletaha D, McInnes IB. Rheumatoid arthritis. Lancet. 2016;388:2023–38. https://pubmed.ncbi.nlm.nih.gov/27156434/
33. Liu G, Lee DP, Schmidt E, Prasad GL. Pathway analysis of global metabolomic profiles identified enrichment of caffeine, energy, and arginine metabolism in smokers but not moist Snuff consumers. Bioinform Biol Insights. 2019;13:1–11. Available from: https://pmc.ncbi.nlm.nih.gov/articles/PMC6798164/.
34. Yu J, Fu J, Zhang X, Cui X, Cheng M. The integration of metabolomic and proteomic analyses revealed alterations in inflammatory-related protein metabolites in endothelial progenitor cells subjected to oscillatory Shear stress. Front Physiol. 2022;13. Available from: https://pmc.ncbi.nlm.nih.gov/articles/PMC8889118/.
35. Xu G, Salen G, Batta AK, Shefer S, Nguyen LB, Niemann W, et al. Glycocholic acid and glycodeoxycholic acid but not glycoursocholic acid inhibit bile acid synthesis in the rabbit. Gastroenterology. 1992;102:1717–23.
36. Sarsenbayeva A, Jui BN, Fanni G, Barbosa P, Ahmed F, Kristófi R et al. Impaired HMG-CoA reductase activity caused by genetic variants or statin exposure: impact on human adipose tissue, β-cells and metabolome. Metabolites. 2021;11. https://pmc.ncbi.nlm.nih.gov/articles/PMC8468287/.
37. Van den Bossche L, Hindryckx P, Devisscher L, Devriese S, Van Welden S, Holvoet, T et al. Ursodeoxycholic acid and its taurine- or glycine-conjugated species reduce colitogenic dysbiosis and equally suppress experimental colitis in mice. Appl Environ Microbiol. 2017;83. Available from: https://pmc.ncbi.nlm.nih.gov/articles/PMC5359499/.
38. Huang K, Liu C, Peng M, Su Q, Liu R, Guo Z, et al. Glycoursodeoxycholic acid ameliorates atherosclerosis and alters gut microbiota in apolipoprotein e–deficient mice. J Am Heart Assoc. 2021;10:19820. https://www.ahajournals.org/doi/abs/https://doi.org/10.1161/JAHA.120.019820
39. Huang F, Pariante CM, Borsini A. From dried bear bile to molecular investigation: a systematic review of the effect of bile acids on cell apoptosis, oxidative stress and inflammation in the brain, across pre-clinical models of neurological, neurodegenerative and neuropsychiatric disorders. Brain Behav Immun. 2022;99:132–46.
40. Huang F. Ursodeoxycholic acid as a potential alternative therapeutic approach for neurodegenerative disorders: effects on cell apoptosis, oxidative stress and inflammation in the brain. Brain Behav Immun Health. 2021;18. Available from: https://pmc.ncbi.nlm.nih.gov/articles/PMC7611783/
41. Nadinskaia M, Maevskaya M, Ivashkin V, Kodzoeva K, Pirogova I, Chesnokov E, et al. Ursodeoxycholic acid as a means of preventing atherosclerosis, steatosis and liver fibrosis in patients with nonalcoholic fatty liver disease. World J Gastroenterol. 2021;27:959–75. https://pubmed.ncbi.nlm.nih.gov/33776366/
42. Moon S-J, Jeong J-H, Jhun JY, Yang EJ, Min J-K, Choi JY, et al. Ursodeoxycholic acid ameliorates pain severity and cartilage degeneration in monosodium iodoacetate-induced osteoarthritis in rats. Immune Netw. 2014;14:45. https://pmc.ncbi.nlm.nih.gov/articles/PMC3942507/.
43. Lee EJ, Kwon JE, Park MJ, Jung KA, Kim DS, Kim EK, et al. Ursodeoxycholic acid attenuates experimental autoimmune arthritis by targeting Th17 and inducing pAMPK and transcriptional corepressor SMILE. Immunol Lett. 2017;188:1–8. https://pubmed.ncbi.nlm.nih.gov/28539269/
44. Matsumoto T, Tsurumoto T. Inappropriate serum levels of IGF-I and IGFBP-3 in patients with rheumatoid arthritis. Rheumatology. 2002;41:352–3. https://doi.org/10.1093/rheumatology/41.3.352
45. Lee H, Suh YS, Lee S, Il, Cheon YH, Kim M, Noh HS, et al. Serum IGF-1 in patients with rheumatoid arthritis: correlation with disease activity. BMC Res Notes. 2022;15. https://pubmed.ncbi.nlm.nih.gov/35382860/

46. Wenwei T, Cheung PT, Lau YL. IGF-I increases interferon-gamma and IL-6 mRNA expression and protein production in neonatal mononuclear cells. Pediatr Res. 1999;46:748–54. https://pubmed.ncbi.nlm.nih.gov/10590034/

Publisher's note